Received: 11 January 2016
DOI: 10.1002/mma.4621

RESEARCH ARTICLE

WILEY

Productivity optimization of microalgae cultivation in a batch photobioreactor process

Héctor Ramírez[1] | Alejandro Rojas-Palma[2] | David Jeison[3]

[1]Departamento de Ingeniería Matemática & Centro de Modelamiento Matemático (CNRS UMI2807), FCFM, Universidad de Chile, Beauchef 851, Santiago, Chile

[2]Departamento de Matemática, Física y Estadística, Facultad de Ciencias Básicas, Universidad Católica del Maule. Avda. San Miguel 3605, Talca, Chile

[3]Escuela de Ingeniería Bioquímica, Pontificia Universidad Católica de Valparaíso. Avda. Brasil 2085, Valparaíso, Chile

Correspondence
Alejandro Rojas-Palma, Departamento de Matemática, Física y Estadística, Facultad de Ciencias Básicas, Universidad Católica del Maule. Avda. San Miguel 3605, Talca, Chile.
Email: amrojas@ucm.cl

Communicated by: J. Muñoz Rivera

Funding information
BASAL PFB-03; Concurso Nacional Tesis de Doctorado en la Empresa (2014), Grant/Award Number: 781413008; CONICYT REDES, Grant/Award Number: 150011; FONDECYT, Grant/Award Number: 1160204; CRHIAM Centre, Grant/Award Number: CONICYT/FONDAP/15130015

MOS Classification: 49J52; 65K05; 90C30; 90C90

We address the question of mean biomass volumetric productivity optimization, which originates from the simplification of dynamics of microalgae in a batch bioreactor process with light incidence. In particular, the stability of the model is analyzed, some optimality necessary conditions for the nonsmooth optimization problem obtained through the inclusion of different photoperiods are studied, and the model is applied in the particular case of *Chlamydomonas reinhardtii* microalgae to validate our results.

KEYWORDS

batch culture, discontinuous differential equation, light/dark cycles, nonsmooth optimization, photobioreactors, volumetric productivity

1 | INTRODUCTION

Bioreactors are laboratory and industrial devices, used for the cultivation of microorganisms. They are usual in a wide variety of applications, including the production of food, beverages, pharmaceutical compounds, polymers, and biofuels. In general terms, a bioreactor can be defined as a container with an inlet to introduce a cultivation media containing substances required for microorganism growth and development, and an outlet through which the produced biomass and products can be extracted. For the most part, devices are also present to enable exchange of gases such as air.

Most industrial scale bioreactors are operated under batch conditions. Thus, the bioreactor is loaded with a cultivation medium and an initial amount of biomass (inoculum), and then cells are allowed to grow for a certain period. Once microorganism concentration reaches a previously specified value, the reactor content is withdrawn, and the unit is prepared for a new operational cycle.[1] The bioreactor characteristics depend largely on the microorganisms that need to be grown. This is clear when we conceive of photobioreactors, which are dedicated to the cultivation of microalgae.[2] A photobioreactor is a bioreactor that incorporates a source light or a disposition enabling exposure to natural solar radiation. Light is necessary to provide the input of photonic energy needed for the photosynthesis process performed by microalgae cells.

Microalgae are recognized as one of the oldest living organisms,[3] are primitive plants (thallophytes), ie, lacking roots, stems, and leaves, have no sterile covering of cells around the reproductive cells, and use chlorophyll as their primary photosynthetic pigment. While the mechanism of photosynthesis in these microorganisms is similar to that of higher plants, they are generally more efficient converters of solar energy because of their simple cellular structure. In addition, because the cells grow in aqueous suspension, they have more efficient access to water, CO_2, and other substrates.[4]

Microalgae can be used for the production of a wide variety of products, including high value compounds (long-chain polyunsaturated fatty acids, vitamins, and pigments) or biofuels (photobiological hydrogen, biodiesel, biomethane, and bioethanol).[4] They can also be used for environmental remediation (carbon dioxide fixation and wastewater treatment). Most of the recent interest that microalgae have received is related to their potential for biofuel production and carbon dioxide fixation based on the impact of these potential applications on the reduction of greenhouse gas emissions.[5] Moreover, their high actual photosynthetic yield compared to terrestrial plants leads to large potential algal biomass production in photobioreactors of several tens of tons per hectare and per year.[6]

The photobioreactor operation is defined by the amount of light that can be provided to microalgae cells, and as biomass concentration increases, optical density of the media also increases, reducing the penetration of light in the culture and thus restricting growth. As a result, growth of microalgae decreases as time proceeds. Then, operational time in batch photobioreactors becomes a key factor determining productivity and the economic feasibility of the process. Optimization of microalgae productivity is then obviously of great interest. In recent years, many works have focused on solutions to this issue via mathematical modelling and optimal control theory.[5,7,8] However, a more practical approach has been realized via experimental studies for specific microalgae species in different environments.[9-11]

In this work, we formulate a microalgae biomass production optimization problem in a photobioreactor in batch mode. In particular, 2 cases are considered separately: constant light incidence and the influence of dark/light cycles.[12] To do this, we propose a simple model based on the well-known Monod growth function, which is widely used in the literature.[13-15] Mathematical results on stability and necessary optimality conditions are given for simplified nonlinear optimization problems based on the general model, and its application was studied in a batch cultivation of the microalgae *Chlamydomonas reinhardtii*.[16]

2 | OPTIMIZATION PROBLEM FORMULATION

2.1 | Model construction

In that follows, we denote by x and s the concentrations of the microorganisms and substrate, respectively, Q_{in} and Q_{out} represent the input and output flows in the bioreactor, respectively, and V represent the volume of the bioreactor.[15]

Assumption 1. The fundamental assumptions considered in the construction of a general mathematical model of the internal dynamics in a bioreactor are

1. The bioreactor vessel is perfectly mixed, that is, the substrate is uniformly distributed.
2. Thus, it is reasonable to assume that what is consumed $c(x, s)$ is proportional to the amount of microorganisms, namely,

$$c(x, s) = \mu(s)Vx, \text{ with } \mu(s) \geq 0 \text{ y } \mu(0) = 0.$$

3. The growth of microorganisms is proportional to what is consumed.
4. Density of the liquid inside the reactor remain constant.

Mass balance equations for xV and sV lead us to write the general model of a bioreactor as follows:

$$\begin{cases} \dfrac{ds}{dt} = \dfrac{Q_{in}}{V}(s_{in} - s) - \dfrac{1}{Y}\mu(s)x, \\ \dfrac{dx}{dt} = \mu(s)x - \dfrac{Q_{in}}{V}x, \\ \dfrac{dV}{dt} = Q_{in} - Q_{out}, \end{cases}$$

where $(s, x, Q_{in}, Q_{out}, V) \in \mathbb{R}^2_{++} \times [0, Q_{max}] \times [0, Q_{max}] \times [0, V_{max}]$ and parameters and functions involved are indicated in Table 1.

The most common growth function is the Monod type (1942)[15,17] (see Figure 1) where μ_{max} represents the maximum specific growth rate of the microorganisms and K_s represents the half saturation coefficient or Michaelis-Menten constant. For the sake of simplicity, we use them in this work.

$$\mu(s) = \mu_{max}\frac{s}{s + K_s}.$$

In the case where $Q_{in} = Q_{out} = 0$, reactor operated under discontinuous or batch mode. Then, the general model reduces to

$$\begin{cases} \dfrac{ds}{dt} = -\dfrac{1}{Y}\mu(s)x, \\ \dfrac{dx}{dt} = \mu(s)x. \end{cases} \tag{1}$$

The idea is to modify the model (1) from the inclusion of certain considerations about the influence of light on the dynamics, which is not considered in the system and including phenomena typical of the microalgae biochemical process.

First, we need to introduce cellular respiration. This is the sum of a series of metabolic processes that enables the microalgae to obtain the biochemical energy required for its growth. This process takes place with or without light. As a result, biomass is converted into CO_2, which is represented by a term $-\rho x$ in the biomass dynamics. The parameter ρ is named *respiration coefficient*. Second, we consider the incident light directly influences the growth rate of microalgae biomass. This is the result of the obvious effect of light over photosynthesis, which represents the primary source of energy for microalgae. Then $\mu = \mu(s, x, I_0(t))$ where $I_0(t)$ represent the time-varying incidental light (see Appendix A).

TABLE 1 Parameters and functions used in the general model

Parameter/Function	Meanings
$\frac{Q_{in}}{V}$	Input rate $[h^{-1}]$
$\frac{Q_{out}}{V}$	Dilution rate $[h^{-1}]$
$\mu(.)$	Growth function $[h^{-1}]$
Y	Yield constant [g cells (g substrate)$^{-1}$]

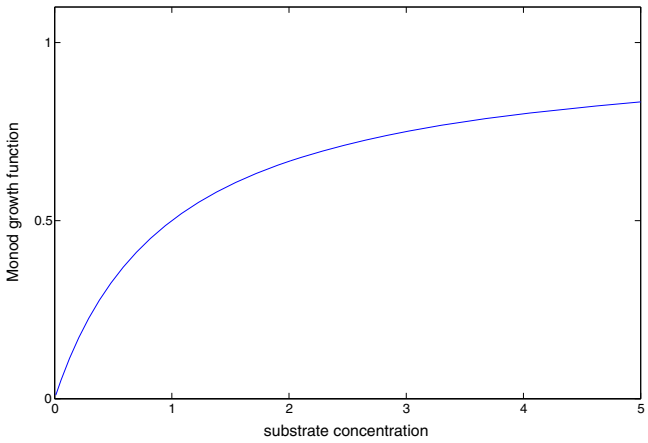

FIGURE 1 Monod growth function [Colour figure can be viewed at wileyonlinelibrary.com]

From the above, the following model is obtained

$$\begin{cases} \dfrac{ds}{dt} = -\dfrac{1}{Y}\mu(s, x, I_0(t))x, \\ \dfrac{dx}{dt} = (\mu(s, x, I_0(t)) - \rho)\, x. \end{cases} \tag{2}$$

Throughout this paper, we consider the following assumptions (see Appendices B and C for details):

Assumption 2. The influence of incidental light $I_0(t)$ is given by

$$I_0(t) = \begin{cases} \bar{I}_0 \text{ if } t_{2k} \le t < t_{2k+1}, & \text{(light phase)}, \\ 0 \text{ if } t_{2k+1} \le t < t_{2k+2}, & \text{(dark phase)}, \end{cases}$$

with $k = 0, 1, \ldots$. This mathematical simplification is enough to analyze the effect of the light in the biomass production.

Assumption 3. The substrate input concentration should always be kept very large so as to always keep the substrate in the region where $s/(s + K_s) \approx 1$. That is, we do not consider substrate limitation during the studied process.

Consequently, growth function μ can be simplified by another similar increasing bounded function $\widetilde{\mu}(x, t) = \frac{\bar{\mu}x(t)}{c+x(t)}$ (considering the obscuration effect over the specific growth rate), and the system (2) is reduced to

$$\frac{dx}{dt} = \frac{\mu(t)\, x}{c + x} - \rho x, \tag{3}$$

defined by a first-order nonlinear differential equation with discontinuous righthand side,[18] where the function $\mu(t)$ can be written as

$$\mu(t) = \begin{cases} \bar{\mu} \text{ if } t_{2k} \le t < t_{2k+1}, & \text{(light phase)}, \\ 0 \text{ if } t_{2k+1} \le t < t_{2k+2}, & \text{(dark phase)}, \end{cases} \tag{4}$$

with $k = 0, 1, \ldots$. In terms of the problem studied, $\mu(t) = \bar{\mu}$ during the light phase (day) and $\mu(t) = 0$ at the dark phase (night). Here, $t_0 > 0$ denote the initial time of the process (See Appendix B for details).

2.2 | Problem statement

The net rate of production determines how much product (volumetric biomass in our case) one can obtain per unit time. So, in the optimization problem, we can use the net rate of production as objective function. The net rate of production for a batch reactor is the quantity of product generated per batch divided by the sum of the final batch process time T and the turnaround time t_a; in case of batch systems, turnaround time will include time taken in forming batches, batch execution, cleaning, and forming a new batch.

The goal then would be to maximize the net rate of production in the photobioreactor in the final batch process time subject to (3) considering 2 different light environments: constant light and dark/light cycles. We can define the objective function to maximize

$$J(x_0, T) = \frac{x(T) - x_0}{T + t_a}. \tag{5}$$

In Equation 5, $J(x_0, T)$ is the net rate of biomass production, $x(T) = x(x_0, T)$ represents the biomass concentration at the end of the batch, $x_0 \ge 0$ represents the biomass concentration at the start of the batch process, $T \ge 0$ is the final batch process time, and $t_a > 0$ is the turnaround time. The function (5) is called *mean biomass volumetric productivity*.[10]

The reactor operator must specify the operating schedule for the operation of the reactor, and this sets the batch processing time. Doing so involves a trade-off that must be considered during the design of a batch reactor and, particularly, during the specification of the operating schedule. Longer operation time implies reduction of productivity due to the optical density of the culture, so biomass reduces its growth when time passes by light obscuration effect. For this reason, an optimization approach is necessary.

The dynamics described by the first-order differential equation in (3) with the objective function defined in (5) are used to define the following optimization problem

$$\max_{(x_0,T)\in\mathbb{R}^2_+} \left\{ J(x_0,T) = \frac{x(x_0,T)-x_0}{T+t_a} \right\}, \tag{6}$$

where $x(x_0,t)$ represents the solution of the discontinuous differential equation 3 with initial condition $x(t_0)=x_0$.

3 | MAIN RESULTS

In this section, we introduce the first results about the problems defined in the previous part, to make a comparison between the optimal values of each case.

3.1 | Constant light

In first place, some results will be shown for the ordinary differential equation

$$\frac{dx}{dt} = \frac{\bar{\mu}x}{c+x} - \rho x, \tag{7}$$

with initial condition $x(t_0)=x_0\in\mathbb{R}_+$.

Remark 4. Since $f(x,t)=\frac{\bar{\mu}x}{c+x}-\rho x$ is continuous as a function with respect to $x\in\mathbb{R}$, for each $(x_0,t_0)\in\mathbb{R}^2$, let $x(x_0,t)$ a solution of the differential equation 7 with initial condition $x(t_0)=x_0$; we have that $x(x_0,t)$ has continuous partial derivatives with respect to x_0[19] and $\frac{\partial x}{\partial x_0}(x_0,t)$ is the solution of the problem (variational equation)[20]

$$\begin{cases} \dot{y} &= \left(\dfrac{\bar{\mu}c}{(c+x)^2}-\rho\right)y, \\ y(t_0) &= y_0. \end{cases}$$

For simplicity, onwards, we denote $x(t)$ a solution of Equation 7 with $x(t_0)=x_0$; however, we will return to the initial condition dependence notation if needed.

Lemma 5. *In the nonlinear differential equation 7, the following holds*

a) The differential equation has a unique solution in the interval $[0,T]$ *with* $T\in\mathbb{R}^+_0$, *and this solution is bounded.*
b) If $\bar{\mu}\le\rho c$, *then the origin is the only equilibrium point and is asymptotically stable for all* $x_0>0$. *Otherwise, if* $\bar{\mu}>\rho c$, *then the origin is unstable, and there is a positive and stable equilibrium point given by* $x^e=\frac{\bar{\mu}}{\rho}-c$.
c) A trajectory $x(t)$ *at the time* $t\in[0,T]$ *is obtained from the implicit equation*

$$\frac{c\ln\left(\frac{x(t)}{x_0}\right)-\frac{\bar{\mu}}{\rho}\ln\left(\frac{\bar{\mu}-\rho(c+x(t))}{\bar{\mu}-\rho(c+x_0)}\right)}{\bar{\mu}-c\rho} = t. \tag{8}$$

Proof. The proof of a) follows directly from existence and uniqueness theorem,[19] where the function $f(x)=\frac{\bar{\mu}x}{c+x}-\rho x$ is Lipschitz continuous with respect the variable x. Its clear also that $M=\max\{x_0,\frac{\bar{\mu}}{\rho}-c\}$ is a bound for this solution.

To prove b) in the first place, we note that the equilibrium points can be obtained by solving the equation

$$\frac{\bar{\mu}x}{c+x}-\rho x=0,$$

whose solutions are $x^0=0$ and $x^e=\frac{\bar{\mu}}{\rho}-c$.

Now, to analyze its stability, we will consider the behavior of solutions for different parameter values. Suppose $\bar{\mu}\le\rho c$, then it follows that at all $x\ge0$

$$\frac{\bar{\mu}x}{c+x}-\rho x\le 0,$$

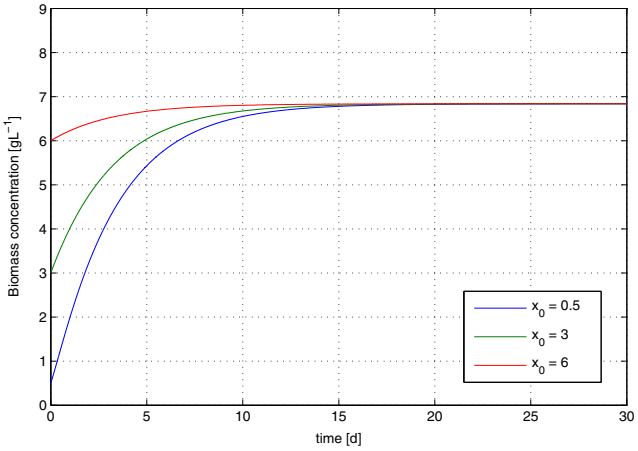

FIGURE 2 Phase plane of the differential equation 7 for microalgae *C reinhardtii* with parameter values $\bar{\mu} = 2.34\ [d^{-1}],\ \rho = 0.34\ [d^{-1}],\ c = 0.253\ [g.L^{-1}]$, and different initial conditions [Colour figure can be viewed at wileyonlinelibrary.com]

with this $\frac{dx}{dt} \leq 0$; in this case, the solution of the differential equation is decreasing in time. Also, the origin is an equilibrium solution, and the uniqueness result above implies $\lim_{t\to\infty} x(t) = 0$. Since we consider only solutions with initial conditions $x(t_0) = x_0 > 0$, it is clear from the above that if $\bar{\mu} \leq \rho c$, the origin is a stable equilibrium point for all initial condition.

Suppose now $\bar{\mu} > \rho c$, we have that if $x_0 > \frac{\bar{\mu}}{\rho} - c$, then

$$\frac{\bar{\mu} x_0}{c + x_0} - \rho x_0 < 0,$$

and $\frac{dx(t_0)}{dt} < 0$. On the other hand, if $x_0 < \frac{\bar{\mu}}{\rho} - c$ using a similar analysis, we have $\frac{dx(t_0)}{dt} > 0$. Then, if $\bar{\mu} > \rho c$, the origin is unstable, and the equilibrium point x^e is stable for any positive initial condition. This result is shown graphically in the phase plane of Figure 2. Finally, c) follows directly from integration, where (7) is separable. □

In this case, $J(x_0, t)$ is continuous and differentiable. Suppose that $\bar{\mu} \leq \rho c$, then $x(x_0, t) - x_0 \leq 0, \forall t \geq 0$, ie, $J(x_0, t) \leq 0, \forall t \geq 0$, and the only possible solution of the optimization problem is the trivial $(x_0, T) = (0, 0)$. So a necessary condition for the existence of a nontrivial solution of the optimization problem (6) is $\bar{\mu} > \rho c$, and this implies $\lim_{t\to\infty} x(t) = x^e$, ie, must exist a positive and stable equilibrium point (which is ensured by Lemma 5).

On the other hand, we can note that $\lim_{t\to\infty} J(x_0, t) = 0$, ie, when there are very large time values, the mean volumetric productivity is dissipated. This means high mean volumetric productivity cannot be achieved at very long periods and implies that the optimal final time of the batch process cannot be very prolonged. Therefore, defining the set

$$\Omega(\tau) = \left\{(x_0, t) \in \mathbb{R}_0^+ \; x_0 \leq x^e, t \leq \tau\right\},$$

for each $\tau > 0$, this set is compact and the Weierstrass extreme value theorem on metric spaces assure the existence of a solution of the optimization problem on this set. From the above, we can find the solution of the optimization problem through the deductive method.[21]

Proposition 6. (Necessary and sufficient conditions for local optimality)

a) (First order) For the optimization problem defined in (6) considering constant light, the pair $\left(x_0^*, T^*\right)$ *is an optimal solution if satisfies*

$$\frac{\partial x}{\partial x_0}(x_0^*, T_0^*) = 1 \quad \textit{and} \quad J(x_0^*, T^*) = f(x(x_0^*, T^*), T^*).$$

b) (Second order) Assuming a), the conditions

$$\frac{\partial^2 x}{\partial x_0^2}(x_0^*, T^*) < 0 \quad \textit{and} \quad \frac{\partial^2 x}{\partial T^2}(x_0^*, T^*) < 0$$

are sufficient to ensure that a maximum is reached at that point.

Proof.

a) The result follows directly from Fermat rule,[21] where $\left(x_0^*, T^*\right)$ must be a critical point of the objective function and therefore must fulfill

$$\nabla_{x_0,T} J(x_0^*, T^*) = 0.$$

In particular,

$$\nabla_{x_0,T} J(x_0, T) = \begin{pmatrix} \frac{\partial J}{\partial x_0} \\ \frac{\partial J}{\partial T} \end{pmatrix}.$$

Now, from the following equalities (stationary conditions)

$$\frac{\partial J}{\partial x_0} = \frac{1}{T + t_a}\left(\frac{\partial x(x_0, T)}{\partial x_0} - 1\right) = 0,$$
$$\frac{\partial J}{\partial T} = \frac{1}{T + t_a}\left(f(x(x_0, T), T) - J(x_0, T)\right) = 0,$$

statement values are obtained.

b) The idea is to use the Hessian condition $H(x_0, T)$ for a maximization problem, which requires that the matrix $H(x_0^*, T^*)$ be negative semidefinite in the critical point (x_0^*, T^*). Evaluating the Hessian in the critical point and assuming that the conditions in part a) are fulfilled

$$H(x_0^*, T^*) = \begin{pmatrix} \frac{1}{T^* + t_a}\frac{\partial^2 x}{\partial x_0^2}(x_0^*, T^*) & 0 \\ 0 & \frac{1}{T^* + t_a}\frac{\partial^2 x}{\partial T^2}(x_0^*, T^*) \end{pmatrix}.$$

If the conditions

$$\frac{\partial^2 x}{\partial x_0^2}(x_0^*, T^*) < 0, \quad \frac{\partial^2 x}{\partial T^2}(x_0^*, T^*) < 0,$$

are satisfied, the Hessian matrix $H(x_0^*, T^*)$ is negative semidefinite, and the critical point $\left(x_0^*, T^*\right)$ satisfies the second-order necessary condition for a local maximum of the optimization problem. □

As shown in Proposition above, with the purpose of find optimal candidates, some nonlinear inequalities must be resolved. However, it is not possible to do explicitly, so it is necessary to implement a numerical algorithm that allows finding an approximation to the problem solution.

3.2 | Dark/light cycles

We now consider some theoretical aspects about the solutions of a nonlinear differential equation with discontinuous righthand side[18]

$$\frac{dx}{dt} = \frac{\mu(t)x}{c + x} - \rho x, \tag{9}$$

where

$$\mu(t) = \begin{cases} \bar{\mu} \text{ if } t_{2k} \le t < t_{2k+1}, & \text{(light phase)} \\ 0 \text{ if } t_{2k+1} \le t < t_{2k+2}, & \text{(dark phase)} \end{cases} \tag{10}$$

for $k = 0, 1, \ldots$, with initial condition $x(0) = x_0$, which is shown in (3) (see Appendix B).

Lemma 7. (Carathéodory solutions)

a) The differential equation with discontinuous righthand side (9) has unique solution in the Caratheodory sense on the interval $[0, T]$ *with* $T \in \mathbb{R}_0^+$.

b) The solutions of (9) in the interval $[0, \tau]$ *with* $\tau > 0$ *have the form*

$$x(t) = \begin{cases} \hat{x}(t) \ \ if \ \ t_{2k} \le t < t_{2k+1}, \\ \hat{x}(t_{2k+1})e^{-\rho(t - t_{2k+1})} \ \ if \ \ t_{2k+1} \le t \le t_{2k+2}, \end{cases}$$

where $0 = t_0 < t_1 < \ldots < t_{2k} < t_{2k+1} < t_{2k+2} < \ldots < \tau$ *and* $\hat{x}(t)$ *is implicitly determined in* $t \in [t_{2k}, t_{2k+1}](k = 0, 1, \ldots)$ *by*

$$\frac{c \ln\left(\frac{\hat{x}(t)}{x(t_{2k})}\right) - \frac{\bar{\mu}}{\rho} \ln\left(\frac{\bar{\mu} - \rho(c + \hat{x}(t))}{\bar{\mu} - \rho(c + x(t_{2k}))}\right)}{\bar{\mu} - c\rho} = t - t_{2k}.$$

Proof.

a) Suppose there exists $b > 0$ such that the function $f(t,x) = \frac{\mu(t)x}{c+x} - \rho x$ is defined on $R = \{(t,x)/t \in [0,a], |x - x_0| \leq b\}$. This is possible, where $x = x(t)$ is bounded on the interval $[0, T]$.
We will prove that the function $f = f(t,x)$ satisfies the 3 Carathéodory's conditions. First, f must be continuous with respect to x for almost everywhere (onwards we will denote a. e.) $t \in \mathbb{R}$. Let $t = t^*$ fixed, the function $f(x) = \mu(t^*)\frac{x}{c+x} - \rho x$ is continuous throughout its domain of definition.
Secondly, the function f is measurable with respect to t for each $x \in \mathbb{R}$. If $t_{2k} \leq t < t_{2k+1}$, then $f(t) = \bar{\mu}\frac{x}{c+x} - \rho x$, which is continuous, and if $t_{2k+1} \leq t < t_{2k+2}$, then $f(t) = -\rho x - Dx$, which is also continuous, ie, there be only discontinuities in t_{2k+i} with $k = 0, 1, \ldots$ and $i = 1, 2, 3, 4$. f is therefore continuous a.e. in t and $[0, T]$ is a Borel set, then f is Lebesgue measurable with respect to t.
Now, it must be

$$\begin{aligned} |f(t,x)| &= \left|\left(\frac{\mu(t)}{c+x} - \rho\right)x\right| \\ &\leq |\frac{\mu(t)}{c} - \rho||x| \\ &= |\frac{\mu(t)}{c} - \rho||x - x_0 + x_0| \\ &\leq |\frac{\mu(t)}{c} - \rho|(b + x_0) \end{aligned}$$

then by defining $m(t) = |\frac{\mu(t)}{c} - \rho|(b + x_0)$, the function $m(t)$ is summable and $|f(t,x)| \leq m(t)$; therefore, f satisfies the Carathéodory conditions in R, which ensures the existence of the solution.
To proof the uniqueness, it is sufficient to prove the generalized Lipschitz condition. Let $(t,x), (t,y) \in R$

$$\begin{aligned} |f(t,x) - f(t,y)| &= \left|\left(\frac{c\mu(t)}{(c+x)(c+y)} - \rho\right)(x - y)\right| \\ &\leq \left|\left(\frac{\mu(t)}{c} - \rho\right)(x - y)\right| \\ &\leq \left|\frac{\mu(t)}{c} - \rho\right||x - y| \end{aligned}$$

namely, $l(t) = \left|\frac{\mu(t)}{c} - \rho\right|$, then l is summable, and this ensures that the solution of the Carathéodory equation 9 exists and is unique.

b) The first part of the proof follows directly from Lemma 5 part c), considering the interval $[t_{2k}, t_{2k+1}]$. The continuity of the solutions at the points $t_{2k+1}(k = 0, 1, \ldots)$ is ensured by Carathéodory conditions proved in part a) above. In particular, any solution is absolutely continuous and satisfies the differential equation except for a measure-zero set. Now, if $t \in [t_{2k+1}, t_{2k+2}]$, Equation 9 is reduced to

$$\begin{cases} \dfrac{dx}{dt} = -\rho x, \\ x(t_{2k+1}) = \hat{x}(t_{2k+1}), \end{cases}$$

which can be solved by separation of variables.

□

Remark 8.

1. When $x(t)$ is a continuous piecewise-defined function, for $k \in \mathbb{N}$ fixed, is easy to show the existence of lateral derivatives

$$D^{-}x(t_{2k+1}) = \lim_{t\to t_{2k+1}^{-}} \frac{x(t)-x(t_{2k+1})}{t-t_{2k+1}} = \frac{\bar{\mu}x(t_{2k+1}) - \rho x(t_{2k+1})(c+x(t_{2k+1}))}{c+x(t_{2k+1})},$$
$$D^{+}x(t_{2k+1}) = \lim_{t\to t_{2k+1}^{+}} \frac{x(t)-x(t_{2k+1})}{t-t_{2k+1}} = -\rho x(t_{2k+1}),$$

analogously, for t_{2k}, we obtain a similar result.

2. We use the definition of stability given by Filippov.[18] A solution $x = \phi(t)$ of a differential equation $\dot{x} = f(t,x)$ is called stable if for each $\epsilon > 0$, there exists $\delta > 0$, which possesses the following property. For each $\tilde{x}_0$ such that $|\tilde{x}_0 - \phi(t_0)| < \delta$, each solution $\tilde{x}(t)$ with the initial data $\tilde{x}(t_0) = \tilde{x}_0$ for $t_0 \le t < \infty$ exists and satisfies the inequality

$$|\tilde{x}(t) - \phi(t)| < \epsilon \ (t_0 \le t < \infty).$$

3. The point $x = p$ is called stationary if it is a trajectory, that is, if $x(t) = p$ is a solution of the differential equation $\dot{x} = f(t,x)$. The term "singular point" is not used here since beside stationary points, we also consider some other singular points, for instance, branching and joining points of trajectories.[18]

Lemma 9. (Stability results)

a) If $\bar{\mu} \ge c\rho$, then the differential equation 9 has stable solutions.
b) If $\bar{\mu} < c\rho$, then the origin is a stable stationary point of the differential equation 9.

Proof.

a) Is necessary to prove that a stable set (not necessarily stationary set) exist. The hypothesis $\bar{\mu} \ge c\rho$ implies that $\frac{dx}{dt} > 0, \forall t \in [t_{2k}, t_{2k+1}]$, ie, $x(t)$ is increasing on this interval. Similarly, $\frac{dx}{dt} < 0, \forall t \in [t_{2k+1}, t_{2k+2}]$, ie, $x(t)$ is decreasing on this interval for $k = 0, 1, \ldots$, this together with the continuity of $x(t)$ implies that $x(t_{2k+1})$ is the maximum value of the function x in the interval $[t_{2k}, t_{2k+2}]$.
If we define the sequence $\{x(t_{2k+1})\}_{k\in\mathbb{N}}$ this sequence is bounded, then Bolzano-Weierstrass Theorem says that there exists a convergent subsequence $\{\bar{x}(t_{2k+1})\}_{k\in\mathbb{N}}$. Let $U = lim_{k\to\infty}\bar{x}(t_{2k+1})$. Using a similar argument, we have that $x(t_{2k+2})$ is the minimum value of the function x in the interval $[t_{2k+1}, t_{2k+3}]$ and we can define the sequence $\{x(t_{2k+2})\}_{k\in\mathbb{N}}$ that is bounded and there exists a convergent subsequence $\{\bar{x}(t_{2k+2})\}_{k\in\mathbb{N}}$. Let $L = lim_{k\to\infty}\bar{x}(t_{2k+2})$. It is clear from the definition of the sequences that $U > L$.
We consider the set $M = [U, L]$ and $dist(y, M) = inf\{d(y, m)/m \in M\}$ the distance from y to the set M, then $dist(\bar{x}(t_{2k+1}), M) \to 0$, $dist(\bar{x}(t_{2k+2}), M) \to 0$ when $k \to \infty$ and this implies that $\forall\epsilon > 0, \exists\delta > 0$ such that for $t_0 \le t < \infty$, each solution $x(t)$ with initial condition $x(t_0) = x_0$ from the δ-neighbourhood of the set M exists and satisfies the inequality $dist(x(t), M) < \epsilon$ and the set M is stable. The oscillatory behavior follows directly from the definition of the function $\mu(t)$ (See Figure 3).

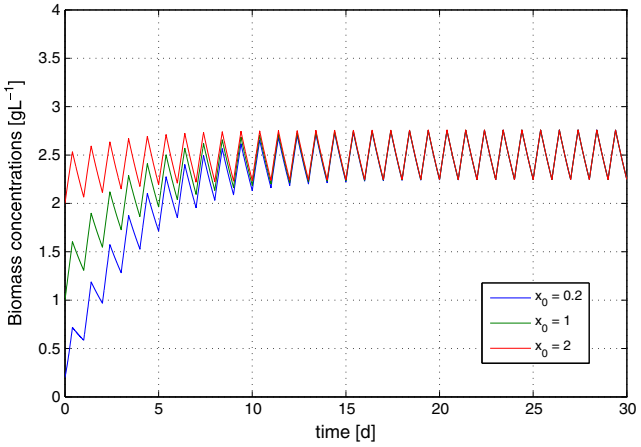

FIGURE 3 Solutions of the differential equation 9 for microalgae *C reinhardtii* with parameter values $\bar{\mu} = 2.34\ [d^{-1}]$, $\rho = 0.34\ [d^{-1}]$, $c = 0.253\ [g.L^{-1}]$, considering regular intervals of 12 hours (0.5 $[d]$) and different initial conditions. A stable set exist in the interior of the interval $[2.35, 2.8]$ over biomass concentration axis [Colour figure can be viewed at wileyonlinelibrary.com]

b) We will use a stability result from direct Lyapunov method for discontinuous differential equations.[18] Let us consider the function

$$v(t,x) = \ln(1+x),$$

then, to check the fulfillment of the stability theorem conditions, it enough guarantee that

$$\frac{dv}{dt} \equiv v_t + \nabla v \cdot f \leq 0, \ |x| < \varepsilon_0, \ (\varepsilon_0 > 0)$$

only in the domains of continuity of the function $f(t,x)$.
Clearly, $v(t,x) \in C^1$, $v(t,0) = 0$, and by the definition of the function, $v(t,x) > 0, \forall x \neq 0$. Now,

$$\begin{aligned} v_t + \nabla v \cdot f &= \frac{\partial v(t,x)}{\partial x} \cdot \frac{dx}{dt} \\ &= \frac{1}{1+x} \cdot \frac{dx}{dt} \\ &= \frac{x}{1+x}\left(\frac{\mu(t)}{c+x} - \rho\right) \\ &< \frac{x}{1+x}\left(\frac{\bar{\mu}}{c} - \rho\right). \end{aligned}$$

From the hypothesis, we have that

$$\frac{\partial v(t,x)}{\partial t} < \frac{x}{1+x}\left(\frac{\bar{\mu}}{c} - \rho\right) < 0, \forall x \neq 0;$$

thus, the function $v(t,x)$ satisfies the condition, and the origin is an stable stationary point. □

The Clarke generalized Jacobian[21] (gradient in our case) of a function g is defined as the convex hull of the B-subdifferential $\partial_B g$, ie, the outer limits of $\nabla g(x,y)$ when $(x_i, y_i) \to (x,y)$ (The meaning is the following: consider any sequence (x_i, y_i) converging to (x,y) while avoiding points at which g is not differentiable and such that the sequence ∇g converges; then the convex hull of all such limit points is ∂g). It is possible to characterize the Clarke generalized gradient in terms of the generalized directional derivatives $J^0((x_0,T);(v_1,v_2))$, in this case,

$$\partial J(x_0,T) = \left\{(x_1,x_2) \in \mathbb{R}^2 : J^0((x_0,T);(v_1,v_2)) \geq \langle (x_1,x_2),(v_1,v_2)\rangle, \forall\ (v_1,v_2) \in \mathbb{R}^2\right\}.$$

Proposition 10. *The function $J(x_0,t) = \frac{x(t)-x_0}{t+t_a}$, where $x(t)$ is the solution of (9) with $x(0) = x_0$ is continuous, locally Lipschitz, and has generalized directional derivatives in all their domain.*

Proof. The continuity is direct from the definition and the continuity of the solution $x(t)$. Let us now see that is locally Lipschitz. In first place, $x(t)$ is locally Lipschitz with respect to t (where $f(t,x)$ defined in lemma 7 is bounded). Now, consider $(x_0,t),(\bar{x}_0,\bar{t}_0) \in \mathbb{R}^2$, then

$$\begin{aligned} |J(x_0,t) - J(\bar{x}_0,\bar{t}_0)| &= \left|\frac{x(t)-x_0}{t+t_a} - \frac{x(\bar{t})-\bar{x}_0}{\bar{t}+t_a}\right| \\ &= \frac{1}{|t+t_a||\bar{t}+t_a|}\left|(x(t)-x_0)(\bar{t}+t_a) - (x(\bar{t})-\bar{x}_0)(t+t_a)\right| \\ &= \frac{1}{|t+t_a||\bar{t}+t_a|}\left|x(t)\bar{t} - x(\bar{t})t + \bar{x}_0 t - x_0\bar{t} + (x(t)-x(\bar{t}))t_a + (\bar{x}_0 - x_0)t_a\right| \\ &\leq \frac{1}{|t+t_a||\bar{t}+t_a|}\left((|\bar{t}| + |x(\bar{t})| + |x_0| + |t_a|)|t-\bar{t}| + (|t| + |t_a|)|x_0 - \bar{x}_0|\right) \\ &\leq K_{x_0,t,\bar{x}_0,\bar{t}}\ \|(x_0,t) - (\bar{x}_0,\bar{t})\| \end{aligned}$$

where

$$K_{x_0,t,\bar{x}_0,\bar{t}} = \frac{\max\{|\bar{t}| + |x(\bar{t})| + |x_0| + |t_a|, |t| + |t_a|\}}{|t+t_a||\bar{t}+t_a|}.$$

Finally, to prove that J has directional derivatives, let $(x_0, t) \in \mathbb{R}^2$, then

$$\begin{aligned}
J^0((x_0,t);(v_1,v_2)) &= \lim_{\substack{(\bar{x}_0,\bar{t})\to(x_0,t)\\ s\to 0}} \frac{J((\bar{x}_0,\bar{t})+s(v_1,v_2))-J(\bar{x}_0,\bar{t})}{s}\\
&= \lim_{\substack{(\bar{x}_0,\bar{t})\to(x_0,t)\\ s\to 0}} \frac{1}{s}\left(\frac{x(\bar{x}_0+sv_1,\bar{t}+sv_2)-(\bar{x}_0+sv_1)}{\bar{t}+sv_2+t_a}-\frac{x(\bar{x}_0,\bar{t})-\bar{x}_0}{\bar{t}+t_a}\right)\\
&= \lim_{\substack{(\bar{x}_0,\bar{t})\to(x_0,t)\\ s\to 0}} \frac{1}{s}\left(\frac{(x(\bar{x}_0+sv_1,\bar{t}+sv_2)-x(\bar{x}_0,\bar{t}))(\bar{t}+t_a)-s((\bar{t}+t_a)v_1+(x(\bar{t})-\bar{x}_0)v_2))}{(\bar{t}+sv_2+t_a)(\bar{t}+t_a)}\right)\\
&= \lim_{(\bar{x}_0,\bar{t})\to(x_0,t)} \frac{\frac{\partial x}{\partial t}(\bar{t}+t_a)v_2+\frac{\partial x}{\partial x_0}(\bar{t}+t_a)v_1-(\bar{t}+t_a)v_1-(x(\bar{t})-\bar{x}_0)v_2}{(\bar{t}+t_a)^2}\\
&= \frac{1}{t+t_a}\left\langle\left(\frac{\partial x}{\partial x_0}-1,\frac{\partial x}{\partial t}-J(x_0,t)\right),(v_1,v_2)\right\rangle.
\end{aligned}$$

Now, where $x(t)$ is differentiable $\forall t \in]t_{2k}, t_{2k+1}[\cup]t_{2k+1}, t_{2k}[$ with $k = 0, 1, 2, \ldots$, then J is differentiable $\forall (x_0, t) \in \mathbb{R}\times]t_{2k}, t_{2k+1}[\cup]t_{2k+1}, t_{2k}[$ and $J^0((x_0,t);(v_1,v_2)) = \nabla J$ in this sets.

Suppose that $(x_0, t_{2k+1}) \in \mathbb{R}\times\{t_{2k+1}\}$ for $k \in \mathbb{N}$ fixed. In these cases, we have to

$$\begin{aligned}
\partial J(x_0,t_{2k+1}) &= \text{co}\left\{\frac{1}{t_{2k+1}+t_a}\begin{pmatrix}\frac{dx(x_0,t_{2k+1})}{dx_0}-1\\ b\end{pmatrix},\frac{1}{t_{2k+1}+t_a}\begin{pmatrix}\frac{dx(x_0,t_{2k+1})}{dx_0}-1\\ a\end{pmatrix}\right\}\\
&= \left\{\frac{1}{t_{2k+1}+t_a}\begin{pmatrix}\frac{dx(x_0,t_{2k+1})}{dx_0}-1\\ y\end{pmatrix} : y\in[a,b]\subset\mathbb{R}\right\},
\end{aligned}$$

(co-represent the convex hull), where

$$\begin{aligned}
a &= -\rho x(t_{2k+1}) - J(x_0,t_{2k+1}),\\
b &= \frac{\bar{\mu}x(t_{2k+1})-\rho(c+x(t_{2k+1}))}{c+x(t_{2k+1})} - J(x_0,t_{2k+1}).
\end{aligned}$$

A similar result is obtained for $(x_0, t_{2k}) \in \mathbb{R}\times\{t_{2k}\}$ for $k \in \mathbb{N}$ fixed. □

Remark 11. From the result above, Rademacher theorem[22] assures that $J(x_0, t)$ is differentiable almost everywhere in $\mathbb{R}^2$ (the set where the function is not differentiable form a set of Lebesgue measure zero). It is $\partial J = \{\nabla J\}$ almost everywhere in $\mathbb{R}^2$, where ∂J represent the Clarke generalized gradient of J.[21]

The problem (6) together with the solution of (9) to (10) is a nonsmooth optimization problem. Recall that a critical point (x_0^*, T^*) of the problem (6) must satisfy

$$\partial J(x_0^*, T^*) \ni 0, \tag{11}$$

where $\partial J(x_0, T)$ represent the Clarke generalized gradient.[21,23]

Proposition 12. (First-order necessary conditions)
An optimal solution (x_0^*, T^*) of (6) satisfies $T^* = t_{2k+1}^*$ for some $k \in \mathbb{N}$ and following conditions

$$i)\ \frac{\partial x}{\partial x_0}(x_0^*, t_{2k+1}^*) = 1,\ \textit{and ii)}\ 0 \in \frac{1}{t_{2k+1}^*+t_a}[a^*, b^*]$$

where $a^* = -\rho x(x_0^*, t_{2k+1}^*) - J(x_0^*, t_{2k+1}^*)$ and $b^* = \frac{\bar{\mu}x(x_0^*,t_{2k+1}^*)-\rho(c+x(x_0^*,t_{2k+1}^*))}{c+x(x_0^*,t_{2k+1}^*)} - J(x_0^*, t_{2k+1}^*)$.
It is noted that the batch process should always end at the end of a period of light.

Proof. If the optimal solution (x_0^*, T^*) is attained in the points where the function is differentiable in the classical sense, when we evaluate the gradient in this point, it should be equal to zero (Euler necessary condition), which does not occur, ie, the candidates to optimal solutions are the critical points $(x_0^*, t_{2k+1}^*) \in \mathbb{R}\times\{t_{2k+1}\}$ for $k = 0, 1, \ldots$, such that $(0, 0)^t \in \partial J(x_0^*, t_{2k+1}^*)$ and from the proposition above

$$\partial J(x_0^*, t_{2k+1}^*) = \left\{ \frac{1}{t_{2k+1}^* + t_a} \left(\begin{array}{c} \frac{dx(x_0^*, t_{2k+1}^*)}{dx_0} - 1 \\ y \end{array} \right) : y \in \left[a, b\right] \subset \mathbb{R} \right\}$$

where

$$a^* = -\rho x(x_0^*, t_{2k+1}^*) - J(x_0^*, t_{2k+1}^*) \text{ and } b^* = \frac{\bar{\mu} x(x_0^*, t_{2k+1}^*) - \rho(c + x(x_0^*, t_{2k+1}^*))}{c + x(x_0^*, t_{2k+1}^*)} - J(x_0^*, t_{2k+1}^*),$$

then, if a critical point (x_0^*, t_{2k+1}^*) is optimum, then it must fulfil the conditions in the statement. □

Where the objective is a nondifferentiable function, it is not possible to apply the classical direct gradient-based methods for resolution of optimization problems (which are quite efficient in general). For this reason, in the next section, we will deal with an approach based on domain discretization.

4 | NUMERICAL APPROACH

Throughout this section, we fix $t_0 = 0$. To solve numerically problem (6), we consider first a turnaround time $t_a = 1$ (in days) and define a grid of values $x_0 \in [0, \bar{x}_0]$, $T \in \left[0, \bar{T}\right]$, with $\bar{x}_0 = \bar{T} = 20$, and step-size $h = 0.1$. For each of these pairs, we obtain $x(T)$ by solving the implicit Equation 8, and then we compute $J(x_0, T)$. This leads to the construction of a surface formed by the triplets $(x_0, T, J(x_0, T))$ for which the maximum of values $J(x_0, T)$ is found by inspection.

4.1 | *C reinhardtii* study case

C reinhardtii is a single cell green alga, belonging to the chlorophytes, a group of highly adaptable species that lives in many different environments throughout the world. *C reinhardtii* usually derives energy from photosynthesis, but thrives in total darkness when provided with an alternative carbon source. *C reinhardtii* has been studied extensively in the past decades. It is regarded as a model organism for green microalgae because of its diverse metabolism and its ability to grow photoautotrophically as well as heterotrophically on acetate. In addition, *C reinhardtii* is able to accumulate starch and produce hydrogen when grown anaerobically.[9]

a) (Constant light) For the algae *C reinhardtii*, we have the following parameter values (see Appendix C) $\bar{\mu} = 2.34\ [d^{-1}]$, $\rho = 0.34\ [d^{-1}]$, $c = 0.253\ [g.L^{-1}]$. For these values, the differential equation 7 has a stable positive equilibrium point in 6.63 $[g.L^{-1}]$ approx. (Lemma 5). Solving (using `fmincon` in `matlab`, for example, or an interior point algorithm), the objective function reaches its maximum value 0.9389 $[g.L^{-1}.d^{-1}]$ and is reached in the initial condition $x_0^* = 0.2\ [g.L^{-1}]$, the terminal time is $T^* = 2.7\ [d]$, ie, in day 3 of the process, the net rate of production is maximized in the case of light constant, starting with a relatively low amount of biomass and the final concentration is $x(T^*) = 3.674\ [g.L^{-1}]$ approx. The pair $(x_0^*, T^*) = (0.2, 2.7)$ satisfies the necessary and sufficient optimality condition (Proposition 6). This case is shown in Figure 4.

b) (Dark/light cycles, summer period) For the same parameter values, but considering Equation 9 in intervals of 14 hours of light (0.6 $[d]$ approx.) and 10 hours of dark (0.4 $[d]$ approx.), the objective function reaches its maximum value 0.6188 $[g.L^{-1}.d^{-1}]$ and is reached in the initial condition $x_0 = 0.3\ [g.L^{-1}]$ and in the terminal time $T = 1.6\ [d]$, ie, between the first and the second day of the process, the net rate of production is maximized in the case of dark/light cycles, starting with a relatively low amount of biomass, but more than in the previous case and the final concentration is $x(T^*) = 1.91\ [g.L^{-1}]$ approx. Since $0 \in [-1.115, 1.164]$, then the optimal values satisfies the first-order optimality condition (Proposition 12). This case is shown in Figure 5.

c) (Dark/light cycles, regular interval) For the same parameter values, but considering the model (9) in regular intervals of 12 hours (0.5 $[d]$), the objective function reaches its maximum value 0.5240 $[g.L^{-1}.d^{-1}]$ and is reached in the initial condition $x_0 = 0.4\ [g.L^{-1}]$ and in the terminal time $T = 1.5\ [d]$, ie, between the first and the second day of the process, the net rate of production is maximized in the case of dark/light cycles, starting with exactly the same amount of biomass that in the previous case and the final concentration is $x(T^*) = 1.7099\ [g.L^{-1}]$ approx. Since $0 \in [-0.506, 0.441]$, then the optimal values satisfies the first-order optimality condition (Proposition 12). This case is shown in Figure 6.

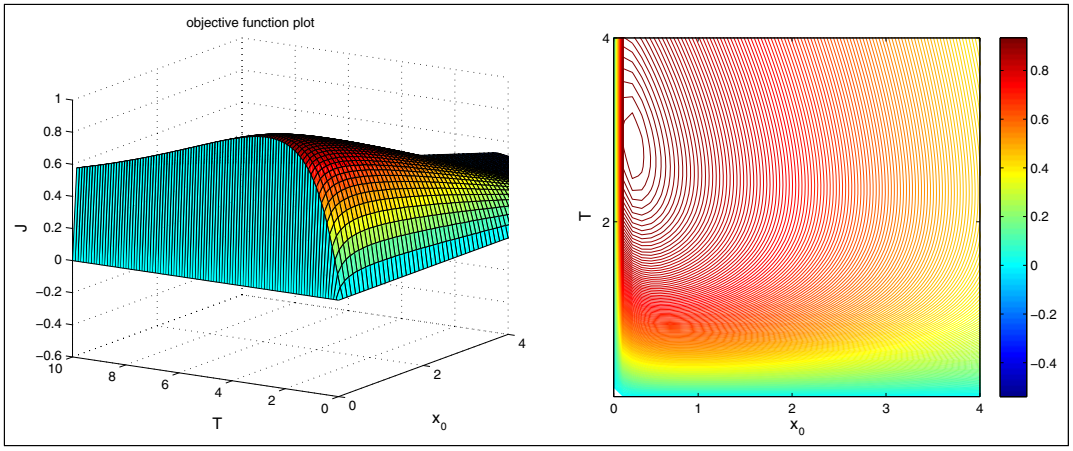

FIGURE 4 Surface and level curves of the net rate of production (mean biomass volumetric productivity) for the optimization problem (6) for *C reinhardtii* at the parameter values $\bar{\mu} = 2.34\ [d^{-1}]$, $\rho = 0.34\ [d^{-1}]$, $c = 0.253\ [g.L^{-1}]$ [Colour figure can be viewed at wileyonlinelibrary.com]

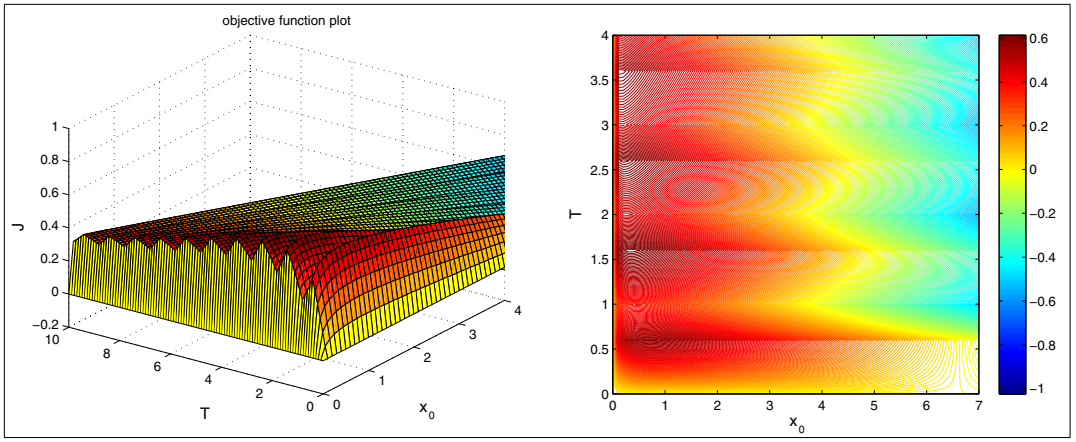

FIGURE 5 Surface and level curves of the net rate of production for the optimization problem (6) for *C reinhardtii* with the same parameter values in summer period [Colour figure can be viewed at wileyonlinelibrary.com]

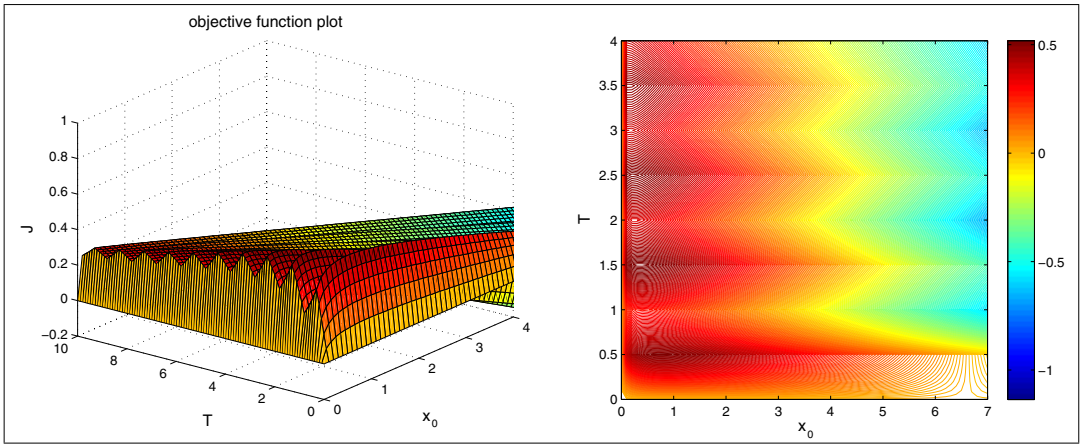

FIGURE 6 Surface and level curves of the net rate of production for the optimization problem (6) for *C reinhardtii* with the same parameter values in regular time intervals [Colour figure can be viewed at wileyonlinelibrary.com]

d) (Dark/light cycles, winter period) For the same parameter values, but considering the model (9) in intervals of 10 hours of light (0.4[d] approx.) and 14 hours of dark (0.6 [d] approx.), the objective function reaches its maximum value 0.4345 [$g.L^{-1}.d^{-1}$] and is reached in the initial condition $x_0 = 0.8\ [g.L^{-1}]$ and in the terminal time $T = 0.4\ [d]$, ie,

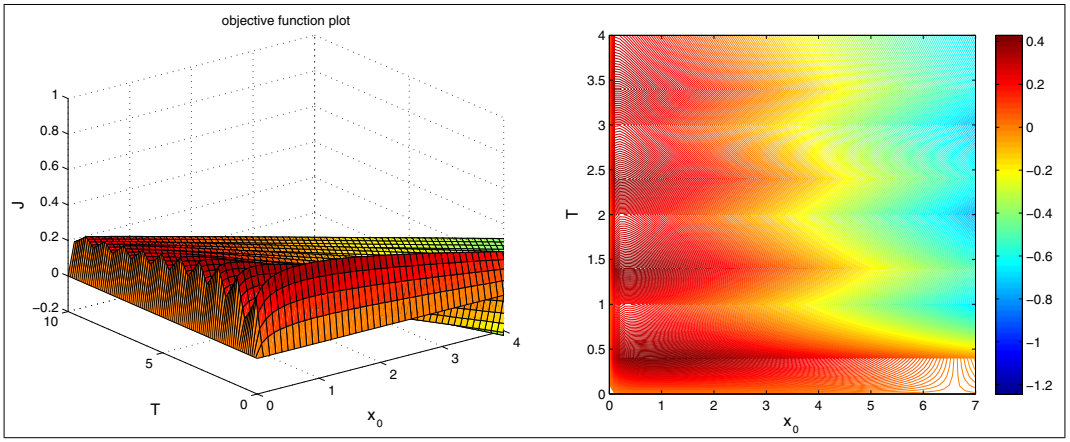

FIGURE 7 Surface and level curves of the net rate of production for the optimization problem (6) for *C reinhardtii* with the same parameter values in winter period [Colour figure can be viewed at wileyonlinelibrary.com]

TABLE 2 Optimal values in different light environments for *C reinhardtii* considering constant light. The optimal trajectories associated to this values are shown in Figure 8

Turnaround time	$t_a = 1$			
Light environment	x_0^* $[gL^{-1}]$	$T^*[d]$	$x(T^*)[gL^{-1}]$	$J^*[gL^{-1}d^{-1}]$
Constant light	0.2	2.7	3.674	0.9389
Summer period [14-10 h]	0.3	1.6	1.91	0.6188
Regular intervals [12 h]	0.4	1.5	1.71	0.5340
Winter period [10-14 h]	0.8	0.4	1.4083	0.4345
Turnaround time	$t_a = 2$			
Constant light	0.1	3.5	4.2475	0.7541
Summer period [14-10 h]	0.2	2.6	2.4017	0.4786
Regular intervals [12 h]	0.2	2.5	1.992	0.3981
Winter period [10-14 h]	0.2	2.4	1.5743	0.3123

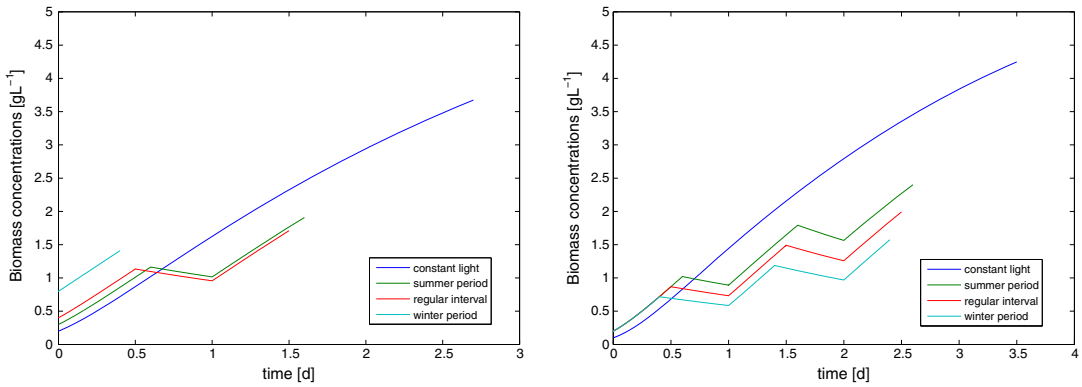

FIGURE 8 Biomass trajectories associated to the optimal values of initial concentration x_0^* and terminal time T^* in different light environments, with turnaround times $t_a = 1$ (left) and $t_a = 2$ (right) [Colour figure can be viewed at wileyonlinelibrary.com]

the first day of the process (during the day, in presence of light), the net rate of production is maximized in the case of dark/light cycles, starting with a relatively high amount of biomass compared to the previous example and the final concentration is $x(T^*) = 1.4083$ $[g.L^{-1}]$ approx. Since $0 \in [-0.913, 1.21]$, then the optimal values satisfies the first-order optimality condition (Proposition 12). This case is shown in Figure 7.

Table 2 resume the results above for different light environments and different turnaround time values.

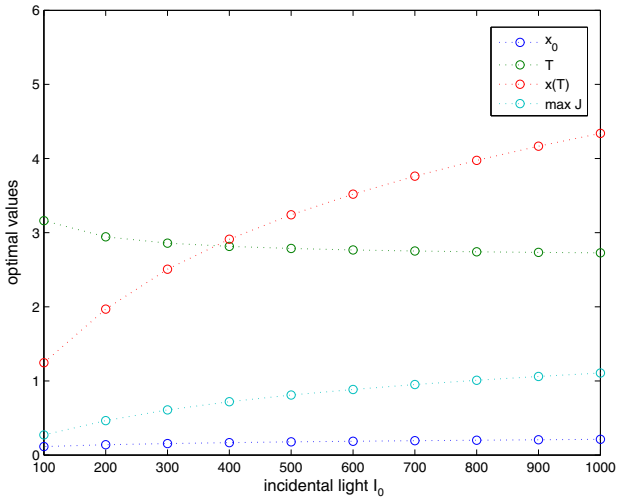

FIGURE 9 The figure shows the results of Table 4. It may be noted that the higher the incidental light, the higher the final biomass concentration, while the terminal batch time decreases and the mean volumetric productivity increases; the initial concentration needed to achieve optimal productivity decreases slightly [Colour figure can be viewed at wileyonlinelibrary.com]

TABLE 3 Parameter estimations for different incidental light settings for *C reinhardtii*

I_0	$\overline{\mu}$	c
1000	2.699	0.2736
900	2.5918	0.2673
800	2.4726	0.2604
700	2.3395	0.2528
600	2.1887	0.2444
500	2.0147	0.2349
400	1.8091	0.2239
300	1.5576	0.2109
200	1.2237	0.1948
100	0.7778	0.1736

TABLE 4 Optimal values in different incidental light settings for *C reinhardtii* considering constant light. This values trends are shown in Figure 9

I_0	x_0^*	T^*	$x(T^*)$	J^*
1000	0.2119	2.7270	4.3397	1.1075
900	0.2062	2.7336	4.1663	1.0607
800	0.2002	2.7424	3.9753	1.0087
700	0.1936	2.7533	3.7620	0.9507
600	0.1862	2.7674	3.5202	0.8849
500	0.1777	2.7866	3.2411	0.8090
400	0.1676	2.8142	2.9110	0.7193
300	0.1554	2.8579	2.5068	0.6095
200	0.1391	2.9442	1.9687	0.4639
100	0.1148	3.1616	1.2454	0.2717

Now, we will consider optimal conditions through varying incidental light; the model parameters are different with respect to the values used in the above simulations (but considering the same measurement units).

For the parameters values in Table 3, we obtain the optimal values in constant light condition using `fmincon` of `Matlab` in the optimization problem (6).

5 | DISCUSSION

In this work a model was formulated based on a batch process in a photobioreactor. From this model, a nonlinear optimization problem was defined, and necessary conditions for maximizing the biomass surface productivity were obtained, subject to the choice of initial biomass microalgae concentration and final operation time. To get analytical results, we try to keep a balance between model simplicity (to handle mathematical analysis) and model complexity to capture the main phenomena that influence a photobioreactor's productivity. We have shown numerically that, because of the day-night behaviour, the productivity rate cannot be as high as it could have been without it (constant light case). However, when the maximal growth rate is sufficiently larger than the respiration rate (for example, in summer period during light phase), we can obtain conditions for which the productivity rate is relatively close to this level.

Three practical points would be nice to highlight, which have been determined from the mathematical analysis in Section 2.3:

1. There is a condition that maximizes productivity, mainly due to the obscuration effect that makes the growth rate decreases with increasing biomass concentration.
2. It is mentioned here that more light (higher intensity or longer period lighting) improve productivity, which is obvious in practice.
3. When operating in natural photoperiods, there is a moment in the day that should harvest the product of the reactor. This is the end of the day, because during the dark period, respiration causes biomass concentration decrease. The result of the optimization problem coincides with this fact.

In the particular case of microalgae *C reinhardtii* estimates of growth parameters and respiration were obtained, the model was applied, and the results were consistent with the previous analysis (Section 2.3). It is interesting that during dark/light cycles in regular intervals, the mean volumetric productivity decreases, being slightly more than half over a 12-hour light photoperiod compared to the case of constant light, and in the same way, the terminal batch time also reduces almost by half in 12-hour photoperiod. Then (in theory) in the same time period in which mean volumetric productivity is maximized in constant light environment, 2 batch processes can be performed at regular intervals (12-hour photoperiod) where, under optimal conditions, higher mean volumetric productivity would be obtained in the addition of both batch process; however, this policy could be not profitable in practice.

By varying the incidental light (and thus the model parameters), small variations are observed in optimal decision variables (x_0^*, T^*) in constant light case, but there exists a difference in the final concentrations and optimal mean volumetric productivity. We can see that the mean volumetric productivity in summer period (14 light hours) and at regular intervals (12 light hours) for incidental light 1000 $[\mu mol.\ m^{-2}.s^{-1}]$ is similar to that obtained in a batch process with constant light with incidental light $400 - 500$ $[\mu mol.\ m^{-2}.s^{-1}]$. In the same way, the final concentrations in these cases are similar; however, the time required to reach this level of productivity would be lower in photoperiods.

ACKNOWLEDGEMENTS

The authors thank Francis Mairet for his fruitful discussions on the topic of this paper. This work is supported by BASAL project PFB-03 (Centro de Modelamiento Matemático, Universidad de Chile), CONICYT PAI grant "Concurso Nacional Tesis de Doctorado en la Empresa" (2014) number 781413008, CONICYT REDES grant 150011 and project BIONATURE of CIRIC, INRIA-Chile. Additionally, the first author is partially supported by FONDECYT project 1160204, and the third author wishes to thank support provided by CRHIAM Centre (CONICYT/FONDAP/15130015).

ORCID

Alejandro Rojas-Palma http://orcid.org/0000-0002-5837-1571

REFERENCES

1. Dunn IJ, Heinzle E, Ingham J, Přenosil JE. *Bioreactor Modelling*. In Biological Reaction Engineering: Dynamic Modelling Fundamentals with Simulation Examples, 2nd ed. Weinheim, FRG: Wiley-VCH Verlag GmbH & Co. KGaA; 2003. https://doi.org/10.1002/3527603050.ch4.
2. Tredici MR, Chini Zittelli G, Rodolfi L. *Photobioreactors*. Encyclopedia of Industrial Biotechnology, Priceton, New Jersey; 1-15.
3. Falkowski P, Raven J. *Aquatic Photosynthesis*, Biology-earth science. Princeton University Press; 2007.
4. Chisti Y. Biodiesel from microalgae. *Biotechnol Adv*. 2007;25:294-306.
5. Masci P, Grognard F, Bernard O. Microalgal biomass surface productivity optimization based on a photobioreactor model. In: 11th IFAC Symposium on Computer Applications in Biotechnology - CAB, Vol. 11. Leuven, Belgique: IFAC; 2010:180-185.
6. Huntley ME, Redalje DG. CO_2 mitigation and renewable oil from photosynthetic microbes: a new appraisal. *Mitigation and Adaptation Strategies for Global Change*. 2007;12(4):573-608.
7. Grognard F, Akhmetzhanov A, Masci P, Bernard O. Optimization of a photobioreactor biomass production using natural light. Proceedings of the 49th IEEE Conference on Decision and Control, CDC. Georgia, USA: IEEE; 2010:4691-4696.
8. Mairet F, Bernard O, Lacour T, Sciandra A. Modelling microalgae growth in nitrogen limited photobiorector for estimating biomass, carbohydrate and neutral lipid productivities. *IFAC World Congress*, Vol. 18. Milano, Italie: IFAC; 2011:10591-10596.
9. Kliphuis AMJ, Klok AJ, Martens DE, Lamers PP, Janssen M, Wijffels RH. Metabolic modeling of Chlamydomonas reinhardtii: energy requirements for photoautotrophic growth and maintenance. *J Appl Phycol*. 2011;24(2):253266.
10. Pruvost J, Vooren GV, Cogne G, Legrand J. Investigation of biomass and lipids production with Neochloris oleoabundans in photobioreactor. *Bioresour Technol*. 2009;100(23):5988-5995.
11. Bertucco A, Beraldi M, Sforza E. Continuous microalgal cultivation in a laboratory-scale photobioreactor under seasonal day-night irradiation: experiments and simulation. *Bioprocess Biosyst Eng*. 2014;37(8):1535-1542.
12. Janssen M, Janssen M, de Winter M, et al. Efficiency of light utilization of Chlamydomonas reinhardtii under medium-duration light/dark cycles. *J Biotechnol*. 2000;78(2):123-137.
13. Bernard O, Gouzé JL. Transient behavior of biological loop models, with application to the droop model. *Math Biosci*. 1995;127(1):19-43.
14. Bernard O. Hurdles and challenges for modelling and control of microalgae for CO_2 mitigation and biofuel production. *J Process Control*. 2011;21(10):1378-1389. Special Issue: Selected Papers From Two Joint {IFAC} Conferences: 9th International Symposium on Dynamics and Control of Process Systems and the 11th International Symposium on Computer Applications in Biotechnology, Leuven, Belgium, July 5-9, 2010.
15. Smith HL, Waltman P. *The Theory of the Chemostat*. New York: Cambridge University Press; 1995. Cambridge Books Online.
16. Harris EH. Chlamydomonas as a model organism. *Annu Rev Plant Physiol Plant Mol Biol*. 2001;52:363-406.
17. Monod J. La technique de la culture continue: Theorie et applications. *Annales de l'Institut Pasteur*. 1950;79:390-410.
18. Filippov AF. *Differential Equations with Discontinuous Righthand Sides: Control Systems*. 1st ed. Dordrecht, The Netherlands: Springer; 1988.
19. Perko L. *Differential Equations and Dynamical Systems*, Texts in Applied Mathematics. Springer Verlag, New York, Inc.: U.S. Government Printing Office; 2001.
20. Hirsch M, Smale S, Devaney R. *Differential Equations, Dynamical Systems, and An Introduction to Chaos*, Differential equations, dynamical systems, and an introduction to chaos. San Diego, California: Academic Press; 2004.
21. Clarke F. *Functional Analysis, Calculus of Variations and Optimal Control*, Graduate Texts in Mathematics. London: Springer; 2013.
22. Clarke F. *Nonsmooth Analysis and Control Theory*, Graduate Texts in Mathematics. Springer, New York: Kluwer Academic Publishers; 1998.
23. Mordukhovich B. *Variational Analysis and Generalized Differentiation I: Basic Theory*, Grundlehren der mathematischen Wissenschaften. Berlin: Springer; 2006.
24. Huisman J, Matthijs H, Visser P, et al. Principles of the light-limited chemostat: theory and ecological applications. *Antonie van Leeuwenhoek*. 2002;81(1-4):117-133.

How to cite this article: Ramírez H, Rojas-Palma A, Jeison D. Productivity optimization of microalgae cultivation in a batch photobioreactor process. *Math Meth Appl Sci*. 2018;41:386–406. https://doi.org/10.1002/mma.4621

APPENDIX A: CONSIDERING LIGHT INCIDENCE

We represent light attenuation following an exponential Beer-Lambert law

$$I(xz) = I_0 e^{-axz}, \tag{A1}$$

where the attenuation at some depth z comes from the total biomass xz per surface unit contained in the layer of depth $[0, z]$, I_0 represents the incident light, and a is a light attenuation coefficient. In microalgae, chlorophyll is mostly the cause of this shadow effect and, in model (1), it is best represented by a fixed portion of the biomass.[13]

Finally, about the light source variation, will be introduced the incident light $I_0 = I_0(t)$ like time-varying. With such an hypothesis on the light intensity that reaches depth z, growth rates vary with depth: In the upper part of the reactor, higher light causes higher growth than in the bottom part.

Following the methodology used in Masci et al[5] for the simplification of the influence of light on the dynamics, supposing that light attenuation directly affects the maximum growth rate,[24] the growth rate for a given depth z can then be written as

$$\mu_z(s, I(xz, t)) = \left(\frac{\tilde{\mu} I(xz, t)}{I(xz, t) + K_I}\right) \frac{s}{s + K_s},$$

with

$$I(xz, t) = I_0(t) e^{-axz}.$$

Based on the above, we can compute the mean growth rate in the reactor

$$\mu(s, I_0(t), x) = \frac{1}{L} \int_0^L \mu_z(s, I(xz, t)) dz,$$

where L is the depth of the reactor and where we have supposed that, even though the growth rate is not homogeneous in the reactor due to the light attenuation, the concentrations of$s$ and x are kept homogeneous through continuous reactor stirring. It is this average growth rate that will be used in the lumped model that we develop.

We then have

$$\begin{aligned}
\mu(s, I_0(t), x) &= \frac{\tilde{\mu}}{L} \int_0^L \left(\frac{I(xz, t)}{I(xz, t) + K_I}\right) dz \frac{s}{s + K_s} \\
&= \frac{\tilde{\mu}}{L} \int_0^L \left(\frac{I_0(t) e^{-axz}}{I_0(t) e^{-axz} + K_I}\right) dz \frac{s}{s + K_s} \\
&= \frac{\widetilde{\mu}}{axL} \ln\left(\frac{I_0(t) + K_I}{I_0(t) e^{-axL} + K_I}\right) \frac{s}{s + K_s},
\end{aligned}$$

Replacing all previously considered in the model (1), we obtain the system

$$\begin{cases}
\dfrac{ds}{dt} = -\dfrac{1}{Y} \dfrac{\tilde{\mu}}{axL} \ln\left(\dfrac{I_0(t) + K_I}{I_0(t) e^{-axL} + K_I}\right) \dfrac{s}{s + K_s} x, \\
\dfrac{dx}{dt} = \dfrac{\tilde{\mu}}{axL} \ln\left(\dfrac{I_0(t) + K_I}{I_0(t) e^{-axL} + K_I}\right) \dfrac{s}{s + K_s} x - \rho x,
\end{cases} \tag{A6}$$

where $\tilde{\mu}$ is hypothetical maximum growth rate, a is a light attenuation coefficient, L is the depth of the reactor, K_I represents the half-saturation coefficient relative to the light,K_s represents the half-saturation coefficient (Michaelis-Menten constant) relative to the substrate, ρ is the respiration rate and all the rest of parameters follows from (1). This model is shown (in a reduced notation form) in (2).

APPENDIX B: SIMPLIFICATION AND REDUCTION OF THE SYSTEM

It seems clear that the larger s translating into large growth rates. In a batch process, the initial substrate concentration should then always be very large so as to always keep the substrate in the region where $\frac{s}{s+K_s} \approx 1$, ie, at such levels that the growth rate only dependent of light influence and biomass at each instant.

Remark 13. The previous hypothesis, which allows a strong simplification of model, is used in Grognard[7] to change and reduce an system similar to (2) to consider in the dynamics of the biomass only the influence of light and thus reduce to a optimal control problem with an independent variable (biomass). In modelling terms, We assume that there is no substrate limitation. This is always true in the initial times in a batch bioreactor, however, in long terms

is not always true. By this reason, high initial substrate concentrations are needed. We assume this hypothesis in our model.

So it can be studied the reduced model

$$\frac{dx}{dt} = \frac{\tilde{\mu}}{axL} \ln\left(\frac{I_0(t) + K_I}{I_0(t)e^{-axL} + K_I}\right) x - \rho x, \tag{B1}$$

which then encompasses all the relevant dynamics for the optimization problem. To more precisely determine the model, we must indicate what the varying light will be like. Classically, it is considered that day light varies as the square of a sinusoidal function so that

$$I_0(t) = \left(\max\left\{\sin\left(\frac{2\pi t}{T_d}\right), 0\right\}\right)^2,$$

where T_d is the length of the day. The introduction of such a varying light would however render the computations analytically untractable. Suppose that the light and dark periods appears in periodic intervals, for $k = 0, 1, \ldots$, and considering $t_0 = 0 < t_1 < \ldots < t_{2k} < t_{2k+1} < \ldots$, we can approximate the light source by a step function:

$$I_0(t) = \begin{cases} \bar{I}_0, & t_{2k} \le t < t_{2k+1}, \quad \text{(light phase)}, \\ 0, & t_{2k+1} \le t < t_{2k+2}, \quad \text{(dark phase)}. \end{cases} \tag{B2}$$

From (B2), the biomass growth in the presence of light is reduced to

$$\mu(I_0(t), x) = \begin{cases} \frac{\tilde{\mu}}{axL} \ln\left(\frac{\bar{I}_0 + K_I}{\bar{I}_0 e^{-axL} + K_I}\right), & t_{2k} \le t < t_{2k+1}, \\ 0, & t_{2k+1} \le t < t_{2k+2}. \end{cases}$$

Finally, we consider a last simplification to the model: instead of considering that the biomass growth in the presence of light has the form

$$\mu_1(x) = \frac{\tilde{\mu}}{axL} \ln\left(\frac{\bar{I}_0 + K_I}{\bar{I}_0 e^{-axL} + K_I}\right) x,$$

which is an increasing and bounded function; following the idea in Grognard et al,[7] we replace $\mu_1(x)$ with another similar increasing bounded function given by

$$\mu_2(x) = \frac{\bar{\mu} x}{c + x},$$

where c is a *fitting parameter* (see Appendix C).

From the simplifications above, the reduced system is

$$\frac{dx}{dt} = \frac{\mu(t)x}{c + x} - \rho x, \tag{B3}$$

where

$$\mu(t) = \begin{cases} \bar{\mu}, & t_{2k} \le t < t_{2k+1} \quad \text{(light phase)}, \\ 0, & t_{2k+1} \le t < t_{2k+2} \quad \text{(dark phase)}. \end{cases} \tag{B4}$$

APPENDIX C: PARAMETER ESTIMATION

To use the model in a case study, we consider algae *Chlamydomonas reinhardtii*. The following table contains parameter values obtained in some references.

For microalgae production is better to use a high incident light. This study was done under oversaturating photon flux density during the light period, $I_0 = 700$ [$\mu mol.\ m^{-2}.s^{-1}$].[12] Now, Kliphuis et al[9] give a respiration rate estimate of 0.53 [$\mu\ mol\ O_2.g^{-1}.h^{-1}$] and a molecular weight of 22.45 [$g.\ molC^{-1}$], and from Falkowski and Raven,[3] the respiratory quotient of this mocroalgae is 1.15 [$molC.\ molO_2^{-1}$]; with these values, we obtain

$$\rho = \frac{0.53 * 1.15 * 22.45}{1000} = 0.014.$$

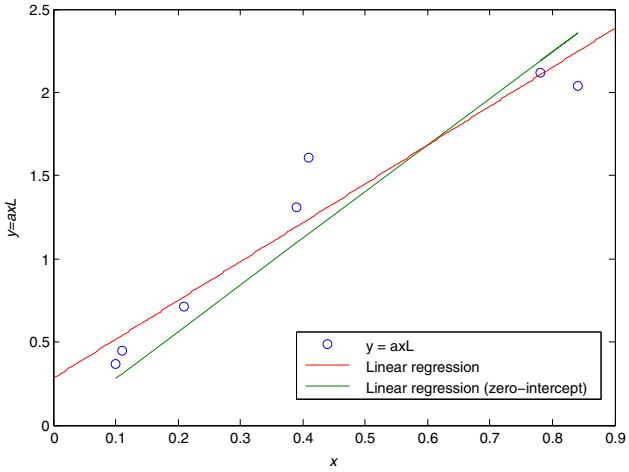

FIGURE C1 Linear regression and zero intercept for the estimation of the light attenuation parameter a [Colour figure can be viewed at wileyonlinelibrary.com]

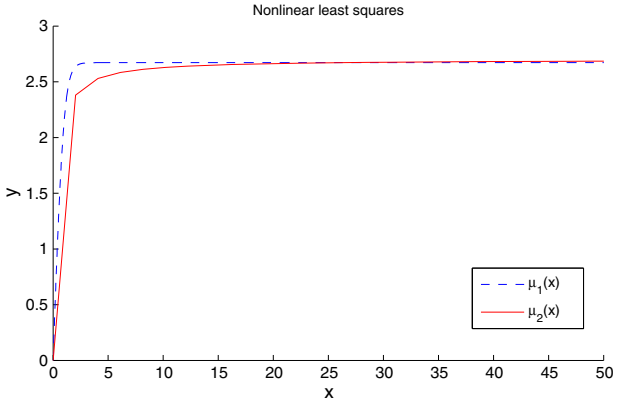

FIGURE C2 Approximation of functions $\mu_1(.)$ and $\mu_2(.)$ by nonlinear least squares method [Colour figure can be viewed at wileyonlinelibrary.com]

TABLE C1 Parameter values for *C reinhardtii* obtained from Janssen et al[12]

Parameter	Value	Units
$\tilde{\mu}$	0.13	h^{-1}
L	0.03	m
K_l	100	$\mu mol.\ m^{-2}.s^{-1}$
$\bar{I}_0$	700	$\mu mol.\ m^{-2}.s^{-1}$

So, in terms of the unit measurement used in this model, the last value is equivalent to $\rho = 0.014\ [h^{-1}]$.

To determine the light attenuation coefficient, we will use a simple linear regression with the data obtained from Kliphuis et al (See Figure C1).[9]

Finally, it is necessary to estimate the last parameters by comparing the functions $\mu_1(x)$ and $\mu_2(x)$ that was defined above (Appendix B) by a nonlinear least squares method (See Figure C2).

In the next table, we showed that the parameters were estimated by the nonlinear least squares method, from the data obtained in references (see Table C1) for the model applied to *C reinhardtii* with corresponding measurement units. Using the same procedure, we can obtain different parameters values for this model, for example, by varying the incidental light I_0 (see Table 3).

TABLE C2 Linear regression $f(x) = axL$

$\mu[h^{-1}]$	$x[g.L^{-1}]$	*I* abs	*I* out	*axL*
0.018	0.78	88	12	2.1203
0.019	0.84	87	13	2.0402
0.031	0.41	80	20	1.6094
0.034	0.39	73	27	1.3093
0.052	0.21	51	49	0.7134
0.061	0.11	36	64	0.4463
0.064	0.1	31	69	0.3711
R^2				0.971
Slope				2.33
Zero-intercept				2.81
a (estimated)	$[m^2.\ g^{-1}]$			0.0933

TABLE C3 Parameters estimated for *C reinhardtii* in this model

Parameter	Value	Units
$\bar{\mu}$	2.34	d^{-1}
ρ	0.34	d^{-1}
c	0.253	$g.L^{-1}$